Multibody System Dynamics **7:** 145–170, 2002.

Modeling and Simulation of Robotic Systems with Closed Kinematic Chains Using the Virtual Spring Approach

JIEGAO WANG, CLÉMENT M. GOSSELIN* and LI CHENG
Département de Génie Mécanique, Université Laval, Québec, Canada G1K 7P4

(Received: 1 August 1999; accepted in revised form: 20 May 2001)

Abstract. The dynamic simulation of robotic or mechanical systems with closed kinematic chains using the virtual spring approach is presented in this paper. This approach uses virtual springs and dampers to include the kinematic constraints thereby avoiding the solution of differential-algebraic equations. A special advantage of this approach is that it leads to a completely decoupled dynamic model which is ideal for real-time dynamic simulation using multi-processor computers. Examples illustrating the approach are given and include the four-bar mechanism with both rigid and flexible links as well as the six-degree-of-freedom Gough–Stewart platform. Simulation results are given for these mechanisms. The results achieve a good agreement with the results obtained from other conventional approaches.

Key words: dynamic simulation, parallel computational algorithms, virtual springs, closed-loop mechanical systems.

1. Introduction

The simulation of robotic manipulators and mechanisms is a very important issue. It can find several applications, for instance, the design of complex systems, virtual environments for operator training, predictive displays for time-delayed teleoperation and the development of advanced robot-control schemes. Numerous researchers have addressed the problem of simulating serial robotic manipulators, see for instance, [1–3, 12, 15, 18, 21, 27] and many other references. By contrast, the simulation of robotic system with closed kinematic chains has received much less attention [5–7, 9]. Dynamic simulation is usually performed in two steps: (1) generation of the dynamic model and (2) solution of the model. The generation of the dynamic models of rigid or flexible manipulators with closed kinematic chains using the principle of virtual work for the computation of the inverse dynamics is thought to be more efficient [22, 26] than using other multibody formulations. However, when used for the solution of the forward dynamics – or

* Author for correspondence, E-mail: gosselin@gmc.ulaval.ca.

dynamic simulation – the solution of the models generated by this approach is not sufficient because there are dependent generalized coordinates in the equations.

Since the dynamic equations of robot manipulators are highly nonlinear and coupled, the analytical solution of such equations is thought to be impossible. Hence, numerical approaches have to be used. Moreover, the forward dynamic solution or dynamic simulation of closed-loop robot manipulators is more difficult than that of serial robot manipulators since the closed-loop constraints cause the dependent coordinates to appear in the dynamic equations and the system is underdetermined. Usually, in order to obtain a determined system, additional equations are obtained by differentiating the constraints. However, the solution of the set of dynamic equations is still not sufficient, because the kinematic constraints in displacements and velocities must be met at the same time. There exist three main methods to include the kinematic constraints of complex robotic mechanisms, namely, (1) the differential-algebraic approach [11], (2) the closed-form kinematic solution approach [14], and (3) the family of formulations referred to as 'force coupling' [20]. However, most of these approaches will lead to complex formulations which are coupled and therefore cannot be directly used for the development of parallel algorithms for real-time dynamic simulation using multi-processors. Indeed, formulations based on DAE and on closed-form solutions consist in assembling a global system of equations in which all degrees of freedom are coupled while formulations based on Lagrange multipliers also require the solution of a global linear system in order to solve for the forces in the constraining joints [13].

In this paper, the generation of the dynamic models of manipulators with closed kinematic chains using virtual springs is revisited. The basic idea of this approach has been used in vibration analysis and in the modeling of constrained mechanical systems [8, 10, 16, 19, 20]. However, it seems that it has not been realized so far that this approach can be used to generate a completely decoupled dynamic model of complex robotic systems with closed kinematic chains and, furthermore, to develop high level parallel algorithms for real-time simulation of these robotic systems. Here, the virtual spring approach is based on the combination of a Lagrangian formulation and virtual springs. It leads to a set of dynamic equations which can be directly used for two purposes, namely, inverse and forward dynamic analysis. When used for inverse dynamic analysis, it leads to the same set of equations of motion as the one obtained using the Lagrange multiplier approach or the principle of virtual work. When used for the simulation or forward dynamic analysis, the dynamic equations obtained from this approach are completely decoupled and automatically include the kinematic constraints. It is ideal for the development of parallel simulation algorithms of robotic manipulators for real-time simulation, which is addressed in detail in other papers [25].

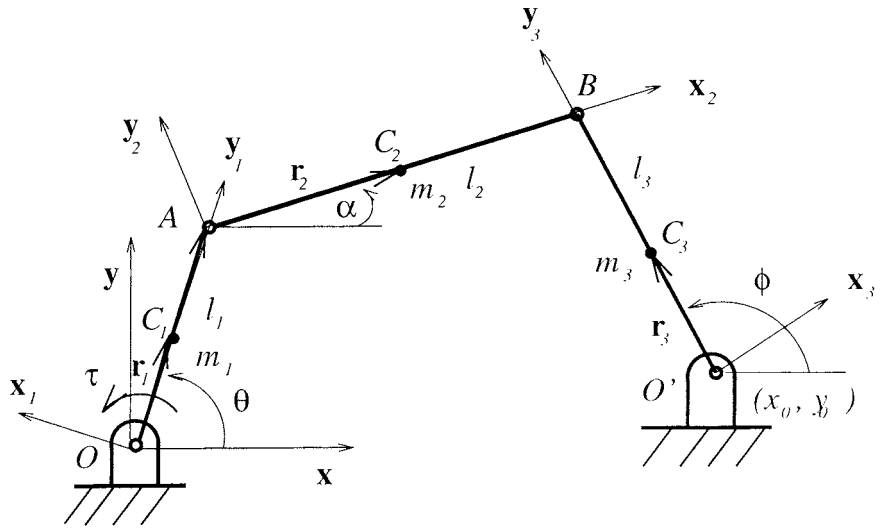

Figure 1. Geometric representation of the four-bar linkage.

2. Generation of Dynamic Models of Closed-Loop Manipulators

The formulation of dynamic models derived from the principle of virtual work or virtual power can be found in [22, 26] and [17]. In this section, the virtual spring approach used to derive the equations of motion of closed-loop manipulators is presented. The set of dynamic equations obtained by this approach are convenient for both purposes: inverse and forward dynamic analysis. In order to illustrate the approach, the derivation of the dynamic equations of a rigid-link four-bar mechanism is first presented and then this approach is applied to the generation of the dynamic model of a spatial six-degree-of-freedom parallel manipulator with prismatic actuators (Gough–Stewart platform).

2.1. DYNAMIC MODEL OF A RIGID-LINK FOUR-BAR MECHANISM USING THE VIRTUAL SPRING APPROACH

The four-bar mechanism is represented in Figure 1. It consists of three movable links. The links of length l_1, l_2 and l_3 are respectively the input link, the coupler link and the output link and their orientation is described respectively by angles θ, α and ϕ. The mass of the moving link with length l_i is m_i and the moment of inertia of the moving link about the axis through the center of mass and perpendicular to the $x_i - y_i$ plane with respect to the moving frame is I_i, where $i = 1, 2, 3$.

A fixed coordinate frame is attached to the base with its origin at the center of the revolute joint connecting the input link to the base. The coordinates of the center point of the revolute joint connecting the output link to the base are (x_0, y_0). A local moving reference frame x_i–y_i $(i = 1, 2, 3)$ is attached to each moving link

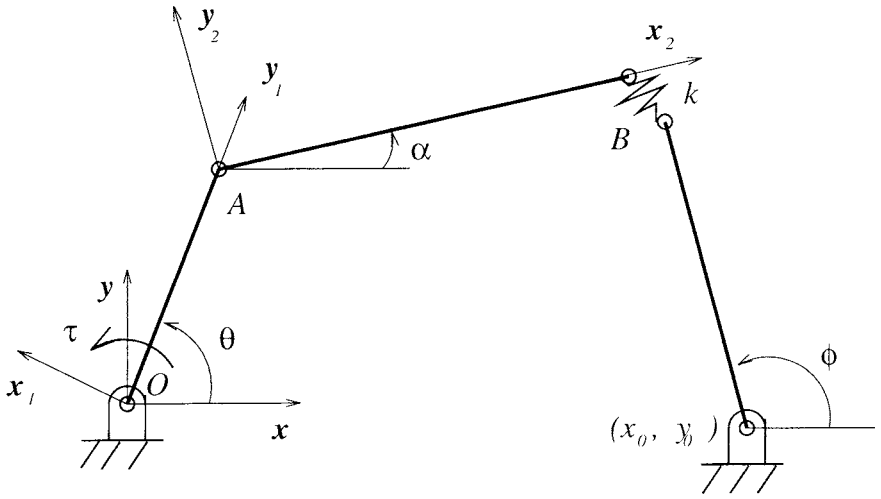

Figure 2. Geometric representation of the equivalent four-bar mechanism.

with its origin located at the center of the revolute joints O, A and O' respectively, as represented in Figure 1.

As mentioned in the introduction, the use of virtual springs to deal with the constraints has first been employed for the study of vibrating systems and constrained mechanical systems. Virtual springs and dampers have also been used for the simulation of serial robots in order to lump link and joint flexibilities [28]. Here, it is proposed to use this approach for the modeling of manipulators or other articulated mechanical systems with closed kinematic loops. The basic idea of this approach is to cut open the closed chains and use virtual springs and dampers to connect the ends of the two links at the open joints. For example, as represented in Figure 2 for the four-bar mechanism, the passive revolute joint at point B is cut open and a spring is used to connect the two links. This operation results in an increase of the degree of freedom of the mechanism. Hence, there are no more dependent variables or generalized coordinates involved in the derivation of the equations of motion of the mechanism. The equations of motion can be derived using a Lagrangian formulation or other mechanics principles by including the elastic potential energy of the spring. When solving the equations of motion, the stiffness of the spring is set to be very large. Theoretically, when the value of the spring stiffness becomes infinitely large, it is equivalent to the ends of the two links being connected by a revolute joint. Therefore the closed-loop constraint is automatically included in the equations of motion.

Cutting the revolute joint B and connecting the coupler link and the output link with a virtual spring of stiffness k, as represented in Figure 2, one can then use a Lagrangian formulation to derive the dynamic equations of the equivalent mechanism.

The position vector of the center of mass of each link can be expressed as

$$\mathbf{r}_{c1} = \mathbf{Q}_1\mathbf{r}_1, \quad \mathbf{r}_{c2} = \mathbf{Q}_1\mathbf{p}_1 + \mathbf{Q}_2\mathbf{r}_2, \quad \mathbf{r}_{c3} = \mathbf{p}_{O'} + \mathbf{Q}_3\mathbf{r}_3, \tag{1}$$

where $\mathbf{Q}_i$ ($i = 1, 2, 3$) is the orientation matrix of the ith link with respect to the base coordinate frame, i.e.,

$$\begin{aligned} \mathbf{Q}_1 &= \begin{bmatrix} \cos\theta & -\sin\theta \\ \sin\theta & \cos\theta \end{bmatrix}, \quad \mathbf{Q}_2 = \begin{bmatrix} \cos\alpha & -\sin\alpha \\ \sin\alpha & \cos\alpha \end{bmatrix}, \\ \mathbf{Q}_3 &= \begin{bmatrix} \cos\phi & -\sin\phi \\ \sin\phi & \cos\phi \end{bmatrix}, \end{aligned} \tag{2}$$

and $\mathbf{r}_1$, $\mathbf{r}_2$ and $\mathbf{r}_3$ are respectively the position vectors from points O, A and O' to the center of mass of the input, coupler and output links

$$\mathbf{r}_1 = \begin{bmatrix} 0 \\ r_1 \end{bmatrix}, \quad \mathbf{r}_2 = \begin{bmatrix} 0 \\ r_2 \end{bmatrix}, \quad \mathbf{r}_3 = \begin{bmatrix} 0 \\ r_3 \end{bmatrix}, \tag{3}$$

while vectors $\mathbf{p}_1$ and $\mathbf{p}_{O'}$ are given as

$$\mathbf{p}_1 = [0 \quad l_1]^T, \qquad \mathbf{p}_{O'} = [x_0 \quad y_0]^T. \tag{4}$$

Differentiating Equation (1) with respect to time, one then obtains the velocities of the center of mass of each link as follows

$$\begin{aligned} \dot{\mathbf{r}}_{c1} &= \begin{bmatrix} -r_1 \sin\theta\,\dot{\theta} \\ r_1 \cos\theta\,\dot{\theta} \end{bmatrix}, \quad \dot{\mathbf{r}}_{c2} = \begin{bmatrix} -l_1 \sin\theta\,\dot{\theta} - r_2 \sin\alpha\,\dot{\alpha} \\ l_1 \cos\theta\,\dot{\theta} + r_2 \cos\alpha\,\dot{\alpha} \end{bmatrix}, \\ \dot{\mathbf{r}}_{c3} &= \begin{bmatrix} -r_3 \sin\phi\,\dot{\phi} \\ r_3 \cos\phi\,\dot{\phi} \end{bmatrix}. \end{aligned} \tag{5}$$

The kinetic energy and gravitational potential energy for the three moving links can now be written as

$$T_1 = \frac{1}{2}m_1(\dot{\mathbf{r}}_{c1}^T\dot{\mathbf{r}}_{c1}) + \frac{1}{2}I_1\dot{\theta}^2 = \frac{1}{2}(I_1 + m_1r_1^2)\dot{\theta}^2, \tag{6}$$

$$\begin{aligned} T_2 &= \frac{1}{2}m_2(\dot{\mathbf{r}}_{c2}^T\dot{\mathbf{r}}_{c2}) + \frac{1}{2}I_2\dot{\alpha}^2 \\ &= \frac{1}{2}m_2l_1^2\dot{\theta}^2 + \frac{1}{2}(I_2 + m_2r_2^2)\dot{\alpha}^2 + m_2l_1r_2\cos(\theta - \alpha)\,\dot{\theta}\,\dot{\alpha}, \end{aligned} \tag{7}$$

$$T_3 = \frac{1}{2}(\dot{\mathbf{r}}_{c3}^T\dot{\mathbf{r}}_{c3}) + \frac{1}{2}I_3\dot{\phi}^2 = \frac{1}{2}(I_3 + m_3r_3^2)\dot{\phi}^2, \tag{8}$$

$$V_1 = m_1g(\mathbf{r}_{c1} \cdot \mathbf{j}) = m_1gr_1\sin\theta, \tag{9}$$

$$V_2 = m_2g(\mathbf{r}_{c2} \cdot \mathbf{j}) = m_2g(l_1\sin\theta + r_2\sin\alpha), \tag{10}$$

$$V_3 = m_3g(\mathbf{r}_{c3} \cdot \mathbf{j}) = m_3g(y_0 + r_3\sin\phi), \tag{11}$$

where $\mathbf{j} = [\,0 \quad 1\,]^T$ is the unit vector along the **y** axis of the base coordinate frame (direction of the gravity field).

The elastic potential energy stored in the virtual spring is expressed as

$$V_s = \frac{1}{2}k||\mathbf{\Delta}||^2, \tag{12}$$

where $\mathbf{\Delta}$ is the displacement vector of the virtual spring, i.e.,

$$\mathbf{\Delta} = \begin{bmatrix} \Delta_x \\ \Delta_y \end{bmatrix} = \begin{bmatrix} l_1\cos\theta + l_2\cos\alpha - l_3\cos\phi - x_0 \\ l_1\sin\theta + l_2\sin\alpha - l_3\sin\phi - y_0 \end{bmatrix}. \tag{13}$$

Therefore, the Lagrangian function can then be obtained as

$$L = \sum_{i=1}^{3}(T_i - V_i) - V_s. \tag{14}$$

By the Lagrange formulation, one finally obtains the dynamic equations for the mechanism

$$\mathbf{M}\ddot{\mathbf{q}} + \mathbf{c}(\dot{\mathbf{q}}, \mathbf{q}) = \mathbf{f}, \tag{15}$$

where $\mathbf{q}$ is the vector of generalized coordinates, $\mathbf{c}(\dot{\mathbf{q}}, \mathbf{q})$ is the vector containing the so-called centrifugal, Coriolis and gravity terms and $\mathbf{f}$ is the vector of elastic forces and actuator forces, i.e.,

$$\mathbf{q} = [\,\theta \quad \alpha \quad \phi\,]^T, \tag{16}$$

$$\mathbf{M} = \begin{bmatrix} I_1 + m_1r_1^2 + m_2l_1^2 & m_2l_1r_2\cos(\theta-\alpha) & 0 \\ m_2l_1r_2\cos(\theta-\alpha) & I_2 + m_2r_2^2 & 0 \\ 0 & 0 & I_3 + m_3r_3^2 \end{bmatrix}, \tag{17}$$

$$\mathbf{c} = \begin{bmatrix} m_2l_1r_2\sin(\theta-\alpha)\,\dot{\alpha}^2 + (m_1gr_1 + m_2gl_1)\cos\theta \\ -m_2l_1r_2\sin(\theta-\alpha)\,\dot{\theta}^2 + m_2gr_2\cos\alpha \\ m_3gr_3\cos\phi \end{bmatrix}, \tag{18}$$

$$\mathbf{f} = \begin{bmatrix} \tau + l_1\sin\theta(k\Delta_x) - l_1\cos\theta(k\Delta_y) \\ l_2\sin\alpha(k\Delta_x) - l_2\cos\alpha(k\Delta_y) \\ -l_3\sin\phi(k\Delta_x) + l_3\cos\phi(k\Delta_y) \end{bmatrix}, \tag{19}$$

where τ is the actuating torque exerted on the input link.

By setting the value of spring stiffness k to be very large, for instance, 10^6, Equation (15) can be used for the simulation or forward dynamic solution of the mechanism. The physical meaning of k is evident, when k is infinity large it is equivalent to a revolute joint connecting the two links. However, when k is too large, the computational efficiency will be abated. In the following numerical example, the choice of the value of k for a specified mechanism will be further discussed. It can be seen that Equation (15) consists of a set of ordinary differential equations and the closed-loop constraints are automatically included in the

equations. The solution of a set of ordinary differential equations should be easier than the solution of differential-algebraic equations.

It can be noticed from Equations (15–19) that the terms $k\Delta_x$ and $k\Delta_y$ actually represent the two components of the vector of the internal forces at joint B and appear to be linear in these equations. Eliminating the two components of internal force, one obtains another form of dynamic equation of this mechanism, which can be used for the computation of the inverse dynamic of the mechanism, i.e.,

$$\begin{aligned}\tau &= (I_1 + m_1 r_1^2 + m_2 l_1^2)\,\ddot{\theta} + m_2 l_1 r_2 \cos(\theta - \alpha)\,\ddot{\alpha} \\ &\quad + m_2 l_1 r_2 \sin(\theta - \alpha)\,\dot{\alpha}^2 + (m_1 g r_1 + m_2 g l_1)\cos\theta \\ &\quad - l_1 \sin\theta\; f_{Bx} - l_1 \cos\theta\; f_{By}, \end{aligned} \tag{20}$$

where

$$\begin{aligned} f_{Bx} &= \big[m_2 r_2 l_1 l_3 \cos\phi \cos(\theta - \alpha)\,\ddot{\theta} + l_3(I_2 + m_2 r_2^2)\cos\phi\,\ddot{\alpha} \\ &\quad + l_2(I_3 + m_3 r_3^2)\cos\alpha\,\ddot{\phi} + m_2 r_2 l_1 l_3 \cos\phi \sin(\alpha - \theta)\,\dot{\theta}^2 \\ &\quad + m_2 g r_2 l_3 \cos\phi \cos\alpha\big]/[l_2 l_3 \sin(\alpha - \phi)], \\ f_{By} &= \big[l_3 m_2 l_1 r_2 \cos(\theta - \alpha)\sin\phi\,\ddot{\theta} + l_3(I_2 + m_2 r_2^2)\sin\phi\,\ddot{\alpha} \\ &\quad + l_2(I_3 + m_3 r_3^2)\sin\alpha\,\ddot{\phi} + m_2 r_2 l_1 l_3 \sin(\alpha - \theta)\sin\phi\,\dot{\theta}^2 \\ &\quad + m_2 g r_2 l_3 \sin\phi\cos\alpha + m_3 g r_3 l_2 \sin\alpha\cos\phi\big]/[l_2 l_3 \sin(\alpha - \phi)]. \end{aligned}$$

Equation (20) is identical to the equation which is obtained if the dynamic model of the four-bar linkage is derived using the principle of virtual work [26]. However, since the accelerations of the links do not need to be computed, the procedure of the derivation given here is simpler and is easy to extend to any multi-degree-of-freedom closed-loop mechanical system.

Another important observation should be made from Equation (17). Indeed, it is noted that the mass matrix is block diagonal, which directly leads to parallelization. It is pointed out that, although the terms $k\Delta_x$ and $k\Delta_y$ represent the constraint forces – which could, for instance, be obtained through Lagrange multipliers – a formulation based on Lagrange multipliers will not lead to such a decoupling since the solution of a global linear system will be required in order to compute the Lagrange multipliers. This decoupling property is the main advantage of the virtual spring method.

In the following subsection, a brief outline of the derivation of the dynamic model of a spatial six-degree-of-freedom manipulator (Gough–Stewart platform) will be presented.

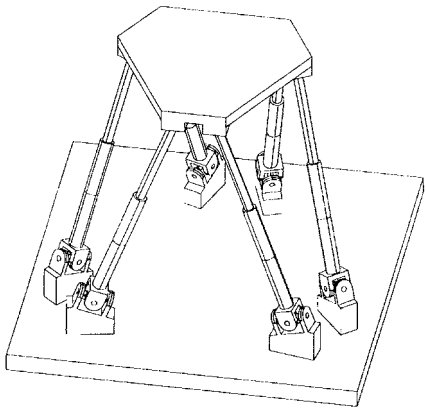

(a) CAD model

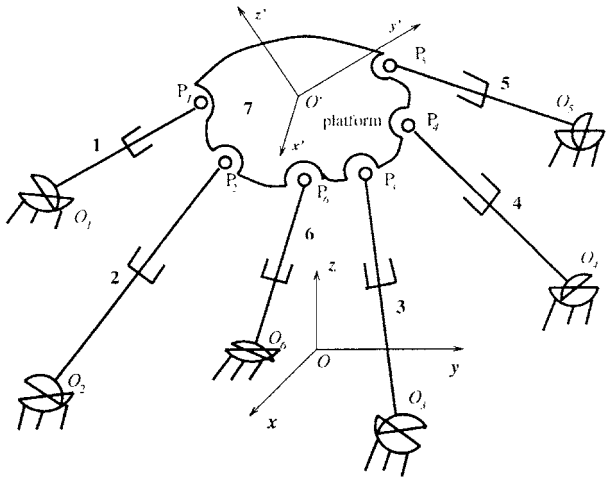

(b) Schematic representation

Figure 3. Spatial six-degree-of-freedom parallel manipulator with prismatic actuators (Gough–Stewart platform).

2.2. DYNAMIC MODEL OF A SPATIAL SIX-DEGREE-OF-FREEDOM PARALLEL MANIPULATOR WITH PRISMATIC ACTUATORS

The spatial six-degree-of-freedom manipulator is represented in Figure 3. It consists of a fixed base and a moving platform connected by six extensible legs. Each extensible leg consists of two links and the two links are connected by a prismatic joint. The moving platform is connected to the legs by spherical joints while the lower end of the extensible legs is connected to the base through Hooke joints. By varying the length of the extensible legs, the moving platform can be positioned and oriented arbitrarily with respect to the base of the manipulator.

The base coordinate frame, designated as the $Oxyz$ frame is attached to the base of the platform with its Z axis pointing vertically upward. Similarly, the moving coordinate frame $O'x'y'z'$ is attached to the moving platform. The orientation of the moving frame with respect to the fixed frame is described by the rotation matrix $\mathbf{Q}$. The center of the ith Hooke joint is noted O_i while the center of the ith spherical joint is noted P_i.

If the coordinates of point P_i in the moving reference frame are noted (a_i, b_i, c_i) and if the coordinates of point O_i in the fixed frame are noted (x_{io}, y_{io}, z_{io}), then one has

$$\mathbf{p}_i = \begin{bmatrix} x_i \\ y_i \\ z_i \end{bmatrix}, \quad \mathbf{p}'_i = \begin{bmatrix} a_i \\ b_i \\ c_i \end{bmatrix}, \quad \text{for } i = 1, \ldots, 6, \quad \mathbf{p} = \begin{bmatrix} x \\ y \\ z \end{bmatrix}, \tag{21}$$

where $\mathbf{p}_i$ is the position vector of point P_i expressed in the fixed coordinate frame – and whose coordinates are defined as (x_i, y_i, z_i) – $\mathbf{p}'_i$ is the position vector of point P_i expressed in the moving coordinate frame, and $\mathbf{p}$ is the position vector of point O' expressed in the fixed frame. One can then write

$$\mathbf{p}_i = \mathbf{p} + \mathbf{Q}\mathbf{p}'_i, \quad i = 1, \ldots, 6, \tag{22}$$

where $\mathbf{Q}$ is the rotation matrix corresponding to the orientation of the platform of the manipulator with respect to the base coordinate frame. This rotation matrix can be written, for instance, as a function of three Euler angles. With the Euler angle convention used in the present work, this matrix is written as

$$\mathbf{Q} = \begin{bmatrix} c_\phi c_\theta c_\psi - s_\phi s_\psi & -c_\phi c_\theta s_\psi - s_\phi c_\psi & c_\phi s_\theta \\ s_\phi c_\theta c_\psi + c_\phi s_\psi & -s_\phi c_\theta s_\psi + c_\phi c_\psi & s_\phi s_\theta \\ -s_\theta c_\psi & s_\theta s_\psi & c_\theta \end{bmatrix}. \tag{23}$$

where s_x denotes the sine of angle x while c_x denotes the cosine of angle x.

The geometric configuration of the ith leg can be represented by spherical coordinate variables, namely, ρ_i, α_i and β_i, as represented in Figure 4, where ρ_i corresponds to the displacement of the ith actuator and $\boldsymbol{\rho}_i$ is the vector from O_i to P_i. Therefore, the configuration of the manipulator can be completely determined by the 24 coordinate variables: x, y, z, ϕ, θ, ϕ, α_i, β_i and ρ_i with $i = 1, \ldots, 6$. These variables are the generalized coordinates of the manipulator and are denoted as

$$\mathbf{q} = [\, x \quad y \quad z \quad \phi \quad \theta \quad \psi \quad \rho_1 \quad \alpha_1 \quad \beta_1 \quad \ldots \quad \rho_6 \quad \alpha_6 \quad \beta_6 \,]^T; \tag{24}$$

$\mathbf{q}$ can be rewritten in another form as

$$\mathbf{q} = [\, \mathbf{q}_p^T \quad \mathbf{q}_1^T \quad \ldots \quad \mathbf{q}_6^T \,]^T, \tag{25}$$

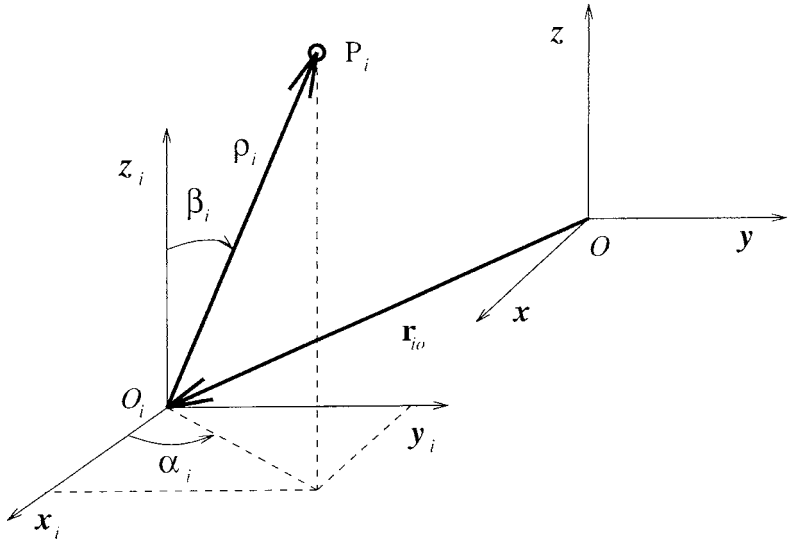

Figure 4. Vector $\boldsymbol{\rho}_i$ in spherical coordinates.

where $\mathbf{q}_p$ and $\mathbf{q}_i$ respectively correspond to the coordinates of the moving platform and the ith leg, namely

$$\mathbf{q}_p = \begin{bmatrix} x \\ y \\ z \\ \phi \\ \theta \\ \phi \end{bmatrix}, \quad \mathbf{q}_i = \begin{bmatrix} \rho_i \\ \alpha_i \\ \beta_i \end{bmatrix}, \quad i = 1, \ldots, 6. \tag{26}$$

In the following, the dynamic model of the manipulator will be derived in terms of these variables.

Similarly, in order to use the virtual spring approach one first needs to open the closed kinematic loops and use a spring to connect them. For example, for the ith leg the spherical joint connecting the leg to the platform is broken and a virtual spring with stiffness k_i $(i = 1, \ldots, 6)$ is used to replace the joint and connect the leg and the platform, as represented in Figure 5. Therefore six virtual springs are applied for the manipulator. Although five springs would be sufficient to open all closed kinematic loops, six springs are used in order to preserve the symmetry of the problem.

The first step of the derivation of the dynamic model is to compute the kinetic energy and potential energy of all links and the elastic potential energy of the virtual springs.

The kinetic energy and potential energy of each link can be respectively expressed as

$$T_p = \frac{1}{2} m_p (\dot{\mathbf{c}}_p^T \dot{\mathbf{c}}_p) + \frac{1}{2} (\boldsymbol{\omega}_p^T \mathbf{I}_p \boldsymbol{\omega}_p)$$

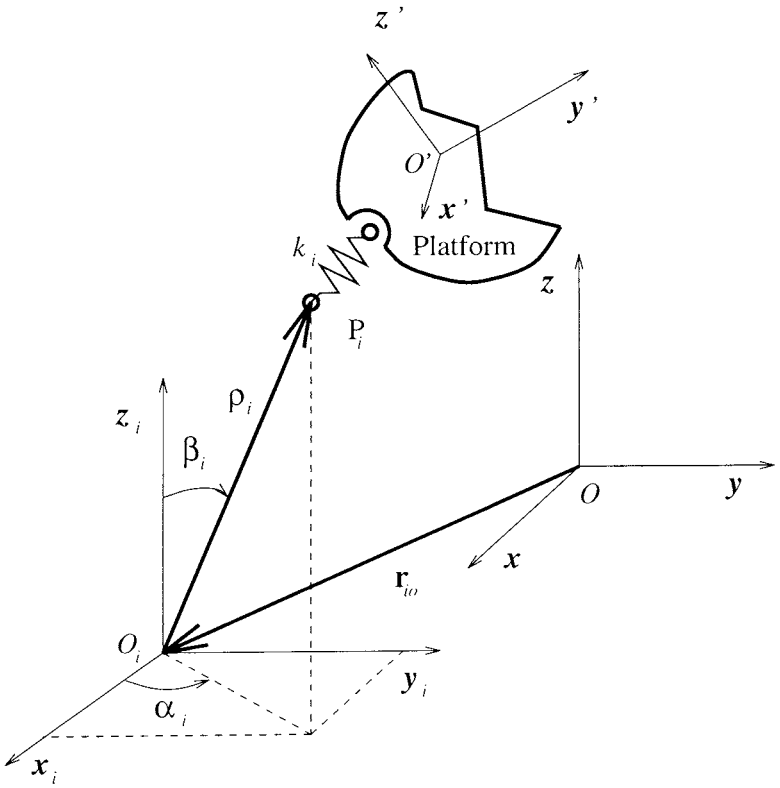

Figure 5. The virtual spring connecting the ith leg to the platform.

$$
\begin{aligned}
&= a_p(\mathbf{q}_p)\,\dot{x}^2 + b_p(\mathbf{q}_p)\,\dot{y}^2 + c_p(\mathbf{q}_p)\,\dot{z}^2 \\
&\quad + d_p(\mathbf{q}_p)\,\dot{\phi}^2 + e_p(\mathbf{q}_p)\,\dot{\theta}^2 + g_p(\mathbf{q}_p)\,\dot{\psi}^2 \\
&\quad + h_p(\mathbf{q}_p)\dot{\phi}\,\dot{\theta} + n_p(\mathbf{q}_p)\dot{\phi}\,\dot{\psi} + l_p(\mathbf{q}_p)\dot{\theta}\,\dot{\psi}, \qquad (27)
\end{aligned}
$$

$$
\begin{aligned}
T_{il} &= \frac{1}{2} m_{il}(\dot{\mathbf{c}}_{il}^T \dot{\mathbf{c}}_{il}) + \frac{1}{2}(\boldsymbol{\omega}_{il}^T \mathbf{I}_{il} \boldsymbol{\omega}_{il}) \\
&= a_{il}(\mathbf{q}_i)\,\dot{\rho}_i^2 + b_{il}(\mathbf{q}_i)\,\dot{\alpha}_i^2 + c_{il}(\mathbf{q}_i)\,\dot{\beta}_i^2 + d_{il}(\mathbf{q}_i)\dot{\rho}_i\,\dot{\alpha}_i \\
&\quad + e_{il}(\mathbf{q}_i)\dot{\rho}_i\,\dot{\alpha}_i + g_{il}(\mathbf{q}_i)\dot{\alpha}_i\,\dot{\beta}_i, \quad i = 1, \ldots, 6, \qquad (28)
\end{aligned}
$$

$$
\begin{aligned}
T_{iu} &= \frac{1}{2} m_{iu}(\dot{\mathbf{c}}_{iu}^T \dot{\mathbf{c}}_{iu}) + \frac{1}{2}(\boldsymbol{\omega}_{iu}^T \mathbf{I}_{iu} \boldsymbol{\omega}_{iu}) \\
&= a_{iu}(\mathbf{q}_i)\dot{\rho}_i^2 + b_{iu}(\mathbf{q}_i)\dot{\alpha}_i^2 + c_{iu}(\mathbf{q}_i)\dot{\beta}_i^2 + d_{iu}(\mathbf{q}_i)\dot{\rho}_i\dot{\alpha}_i \\
&\quad + e_{iu}(\mathbf{q}_i)\dot{\rho}_i\dot{\alpha}_i + g_{iu}(\mathbf{q}_i)\dot{\alpha}_i\dot{\beta}_i, \quad i = 1, \ldots, 6, \qquad (29)
\end{aligned}
$$

$$
V_p = m_p g(\mathbf{c}_p \cdot \mathbf{k}) = m_p g\, u_p(\mathbf{q}_p), \qquad (30)
$$

$$V_{il} = m_{il} g(\mathbf{c}_{il} \cdot \mathbf{k}) = m_{il} g\, u_{il}(\mathbf{q}_i), \quad i = 1, \ldots, 6, \tag{31}$$

$$V_{iu} = m_{iu} g(\mathbf{c}_{iu} \cdot \mathbf{k}) = m_{iu} g\, u_{iu}(\mathbf{q}_i), \quad i = 1, \ldots, 6, \tag{32}$$

where T_p, T_{il} and T_{iu} are respectively the kinetic energy of the platform, the first link and the second link of the ith leg while V_p, V_{il} and V_{iu} are their potential energy. Expressions of the type $x(\mathbf{q}_p)$ and $y(\mathbf{q}_i)$ denote that the coefficients x and y are respectively functions of the generalized coordinates $\mathbf{q}_p$ and $\mathbf{q}_i$. Vectors $\mathbf{c}_x$ and $\boldsymbol{\omega}_x$ are respectively the position vector of the center of mass and the vector of angular velocity of the link x. Finally, $\mathbf{k}$ is a unit vector along the direction of $\mathbf{z}$ axis (direction of the gravity field).

The elastic potential energy stored in the ith virtual spring can be written as

$$V_{is} = \frac{1}{2} k_i ||\boldsymbol{\Delta}_i||^2 = u_s(\mathbf{q}_p, \mathbf{q}_i), \quad i = 1, \ldots, 6, \tag{33}$$

where $\boldsymbol{\Delta}_i$ is the vector of the displacement corresponding to ith virtual spring

$$\boldsymbol{\Delta}_i = \mathbf{p}_{ip} - \mathbf{p}_{il} = \begin{bmatrix} \Delta_{ix} \\ \Delta_{iy} \\ \Delta_{iz} \end{bmatrix}, \quad i = 1, \ldots, 6 \tag{34}$$

and

$$\mathbf{p}_{ip} = \mathbf{p} + \mathbf{Q}\mathbf{p}'_i, \quad i = 1, \ldots, 6, \tag{35}$$

$$\mathbf{p}_{il} = \mathbf{r}_{i0} + \boldsymbol{\rho}_i, \quad i = 1, \ldots, 6, \tag{36}$$

where $\mathbf{r}_{i0}$ and $\boldsymbol{\rho}_i$ are defined in Figure 5.

The Lagrangian function for the six-degree-of-freedom manipulator can therefore be obtained as

$$L = T_p + \sum_{i=1}^{6} (T_{il} + T_{iu}) - [V_p + \sum_{i=1}^{6} (V_{il} + V_{iu} + V_{is})]. \tag{37}$$

Finally, by the application of the Lagrange formulation, one can obtain the dynamic equations of the manipulator as

$$\mathbf{M}\ddot{\mathbf{q}} + \mathbf{g}(\dot{\mathbf{q}}, \mathbf{q}) = \mathbf{f}(\mathbf{q}, t), \tag{38}$$

where $\mathbf{M}$ is a 24×24 inertia matrix, $\mathbf{g}(\dot{\mathbf{q}}, \mathbf{q})$ contains the nonlinear terms, $\mathbf{f}(\mathbf{q}, t)$ contains the spring and actuator forces and $\mathbf{q}$ is the vector of generalized coordinates defined in Equation (24), i.e.,

$$\mathbf{M} = \begin{bmatrix} \mathbf{M}_{p1} & & & & & & & \\ & \mathbf{M}_{p2} & & & & & & \\ & & \mathbf{M}_{l1} & & & \mathbf{0} & & \\ & & & \mathbf{M}_{l2} & & & & \\ & & & & \mathbf{M}_{l3} & & & \\ & & \mathbf{0} & & & \mathbf{M}_{l4} & & \\ & & & & & & \mathbf{M}_{l5} & \\ & & & & & & & \mathbf{M}_{l6} \end{bmatrix}. \tag{39}$$

Numerical problems may occur when using springs to include the kinematic constraints. Since the stiffness of the ith virtual spring k_i has to be very large, the damping problem will become more evident with the increase of k_i, and hence the velocity constraint may not be met very well. In order to eliminate the underdamping effect, internal damping forces are added to Equation (38). This term is related to the generalized velocities and displacements and can be expressed as

$$\mathbf{d}(\dot{\mathbf{q}}, \mathbf{q}) = \begin{bmatrix} \sum_{i=1}^{6} b_i \dot{\boldsymbol{\Delta}}_i^T (\frac{\partial \boldsymbol{\Delta}_i}{\partial \mathbf{q}_1}) \\ \sum_{i=1}^{6} b_i \dot{\boldsymbol{\Delta}}_i^T (\frac{\partial \boldsymbol{\Delta}_i}{\partial \mathbf{q}_2}) \\ \vdots \\ \sum_{i=1}^{6} b_i \dot{\boldsymbol{\Delta}}_i^T (\frac{\partial \boldsymbol{\Delta}_i}{\partial \mathbf{q}_6}) \end{bmatrix}, \tag{40}$$

where b_i $(i = 1, \ldots, 6)$ is the damping coefficient of the ith virtual spring and $\dot{\boldsymbol{\Delta}}_i$ denotes the time derivative of the assumed displacement vector of ith virtual spring $\boldsymbol{\Delta}_i$.

Therefore, Equation (38) should be rewritten as

$$\mathbf{M}\ddot{\mathbf{q}} + \mathbf{g}(\dot{\mathbf{q}}, \mathbf{q}) + \mathbf{d}(\dot{\mathbf{q}}, \mathbf{q}) = \mathbf{f}(\mathbf{q}, t). \tag{41}$$

The solution of the forward dynamics consists in solving the following linear system for $\ddot{\mathbf{q}}$

$$\mathbf{M}\ddot{\mathbf{q}} = \mathbf{f}(\mathbf{q}, t) - \mathbf{b}, \tag{42}$$

where

$$\mathbf{b} = \mathbf{g}(\dot{\mathbf{q}}, \mathbf{q}) + \mathbf{d}(\dot{\mathbf{q}}, \mathbf{q}). \tag{43}$$

Moreover, it can be noticed from Equation (39) that the inertia matrix is a block diagonal matrix, which implies that the solution of the forward dynamics can be implemented separately by different processors. For instance, eight processors can be used in this case and will result in much faster solution, which is a prerequisite for real-time simulation. Therefore, the dynamic models derived using the virtual spring approach are ideal for real-time dynamic simulation using parallel computers.

When applied to the computation of the inverse dynamics of the manipulator, Equations (38) can be reduced to a system with six equations by eliminating the internal action forces: $k_i \Delta_{ix}$, $k_i \Delta_{iy}$ and $k_i \Delta_{iz}$ $(i = 1, \ldots, 6)$. Solving the linear system for τ_i, one finally obtains the formulations of inverse dynamics for the manipulator.

3. Simulation of Mechanical Systems with Closed Kinematic Chains

The solution of the forward dynamics of closed-loop mechanical systems with closed kinematic chains is much more difficult than that of open chain mechanical

systems. Because of the kinematic constraint problem, the solution of a set of ordinary differential dynamic equations is not sufficient, the constraints have to be included. As mentioned above, there exist several main approaches to deal with the kinematic constraint problems, namely, differential-algebraic (DAE) approach [20], closed-form kinematic solution approach and the virtual spring approach [20, 24, 25] (also called force coupling approach [20]). The differential-algebraic approach and closed-form kinematic solution approach might be more efficient than the virtual spring approach for the simulation of simple and small systems. However, they cannot lead to a completely decoupled formulation. By contrast, as presented above, the dynamic equations derived using the virtual spring approach can be completely decoupled, namely, the mass matrices are block diagonal, which allows one to develop real-time simulation algorithms using multi-processors at a high level.

In this section, the simulation of three types of mechanisms with closed kinematic loops is implemented using the formulations derived from the virtual spring approach. The simulation of the four-bar mechanisms with both rigid and flexible links is firstly presented and the results are compared with the results obtained from other approaches. Then, the simulation of the Gough–Stewart platform using parallel algorithms is performed. It can be noticed that the modeling and simulation of complex robotic systems with closed kinematic chains using the virtual spring approach leads to a parallel algorithm and will be easily to be implemented in multi-processor computer systems.

3.1. SIMULATION OF A RIGID-LINK FOUR-BAR MECHANISM

In this subsection, the simulation of a rigid-link four-bar mechanism is performed using the three approaches mentioned above and the results obtained are then compared.

It is assumed that the link parameters of the mechanism are given as

$$l_1 = 1, \quad l_2 = 4, \quad l_3 = 2.5,$$

$$m_i = 1, \quad r_i = l_i/2 \quad (i = 1, 2, 3),$$

$$x_0 = 3, \quad y_0 = 0, \quad g = 9.8,$$

where the lengths are given in meters and the masses in kilograms.

The moment of inertia can be computed using $I_i = (m_i l_i^2)/12$ $(i = 1, 2, 3)$ and an actuating torque $\tau = 6$ is exerted on the input link, with initial conditions

$$\theta = \pi/2, \quad \alpha = 0.353281, \quad \phi = 1.26486,$$

$$\dot{\theta} = 0, \quad \dot{\alpha} = 0, \quad \dot{\phi} = 0,$$

where the angles are in radians.

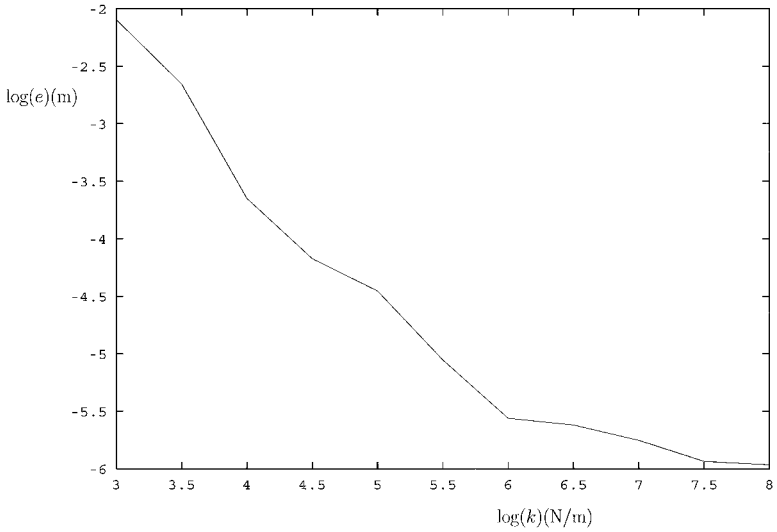

Figure 6. The position error with respect to the different value of k.

3.1.1. *Simulation Using the Virtual Spring Approach*

Letting $k = 10^6$ in Equation (15) and using a MAPLE's ODE solver: the fourth-fifth order Runge–Kutta method with default values for the relative and absolute error tolerances, one obtains the forward dynamic solution of the rigid-link four-bar mechanism during the first two seconds, as represented in Figure 7. It is pointed out here that the choice of the numerical value of the stiffness k will have a significant effect on the accuracy and the computational speed. Theoretically, the largest possible value of k should lead to the best results. However, a too large value of k will result in not only the reduction of the computational speed but also probable ill-conditioning of the dynamic equations. A way to choose the value of k is to plot the curve of the position error of the mechanism in terms of different values of k at a specified time. For instance, at $t = 0.1$ second, one can compute the position error, e, using different values of k as

$$e = \sqrt{\Delta_x^2 + \Delta_y^2}, \tag{44}$$

where Δ_x and Δ_y are defined in Equation (15). The error curve is shown in Figure 6. It can be seen that the error significantly decreases with the increasing of the spring stiffness. When $\log(k) = 6$, namely, $k = 10^6$, the value of e is around $10^{-5.5}$, which means that the position constraint can be met very well.

Actually, the example presented here also shows that when $k = 10^6$ the results are in good agreement with those obtained using other approaches and the computational speed is ideal in comparison with other approaches.

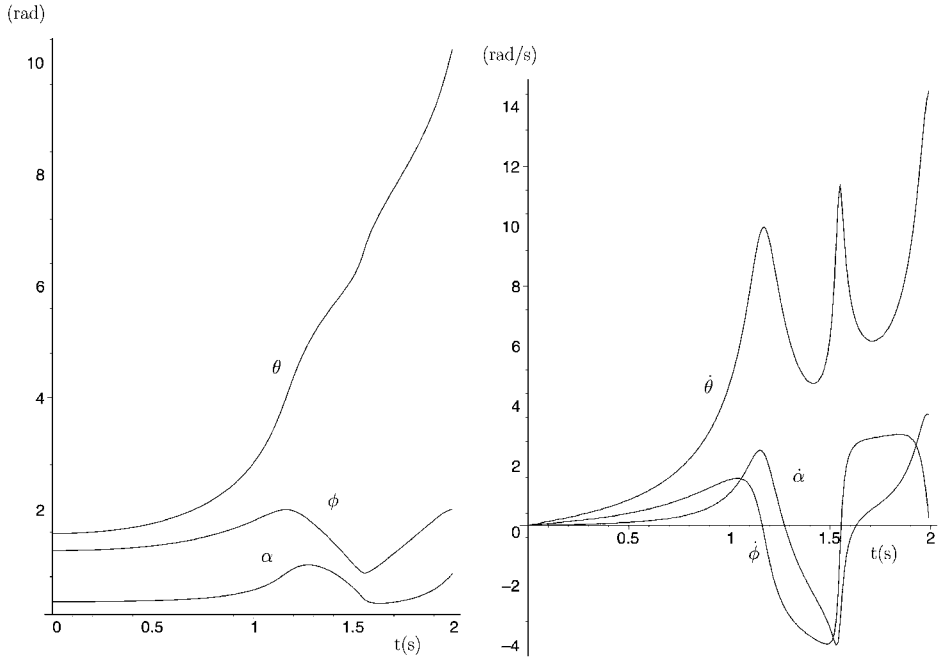

(a) Angular displacements θ, α and ϕ (rad) (b) Angular velocities $\dot{\theta}$, $\dot{\alpha}$ and $\dot{\phi}$ (rad/s)

Figure 7. The angular displacement and velocity of the three links of the rigid-link four-bar mechanism.

3.1.2. *Comparison of the Results*

Using the DAE approach and the closed-form kinematic solution approach for the rigid-link four-bar mechanism leads to almost identical results. Moreover, the difference between the results obtained with the virtual spring approach and those obtained from the other two approaches is very small, as evidenced by the error plots shown in Figure 8.

3.2. SIMULATION OF A FOUR-BAR MECHANISM WITH A FLEXIBLE LINK

3.2.1. *Simulation Using the Virtual Spring Approach*

(I) *Derivation of the dynamic model*

In this section, the simulation of a four-bar mechanism with a flexible coupler link using the virtual spring approach is performed and then the results obtained are compared with those obtained from the approach using the converted ordinary differential equations (ODE).

The virtual spring approach is particularly advantageous in the presence of flexible links. In fact, when using the classical Rayleigh–Ritz method, the admissible functions should satisfy the continuity between each of the adjacent links, which

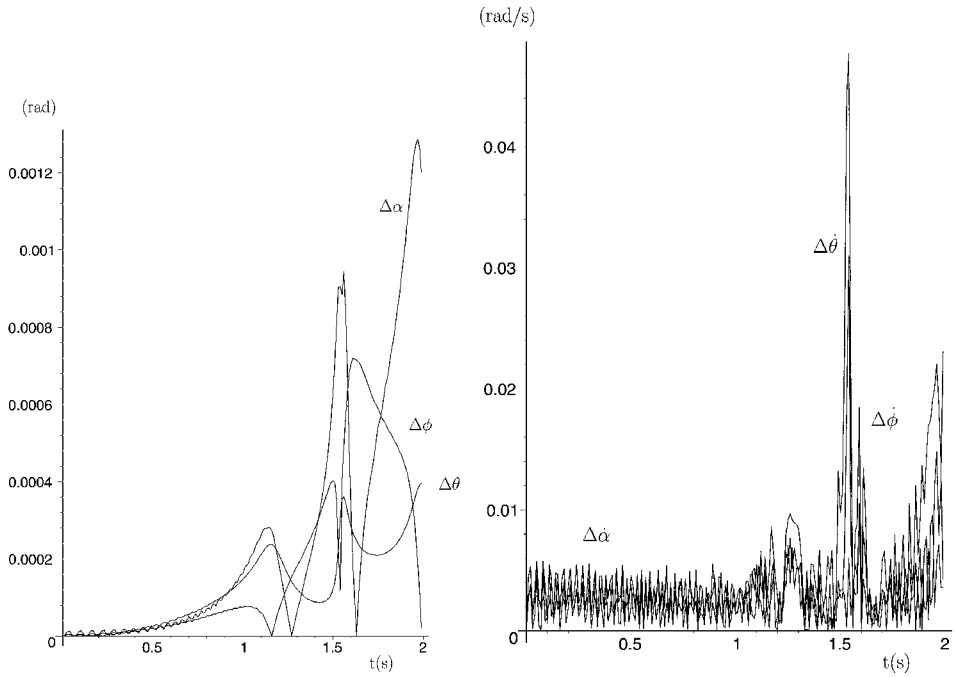

(a) Displacements errors $\Delta\theta$, $\Delta\alpha$ and $\Delta\phi$ (rad) (b) Velocities errors $\Delta\dot{\theta}$, $\Delta\dot{\alpha}$ and $\Delta\dot{\phi}$ (rad/2)

Figure 8. The error curves of the displacement and velocity of the three links of the rigid-link four-bar mechanism.

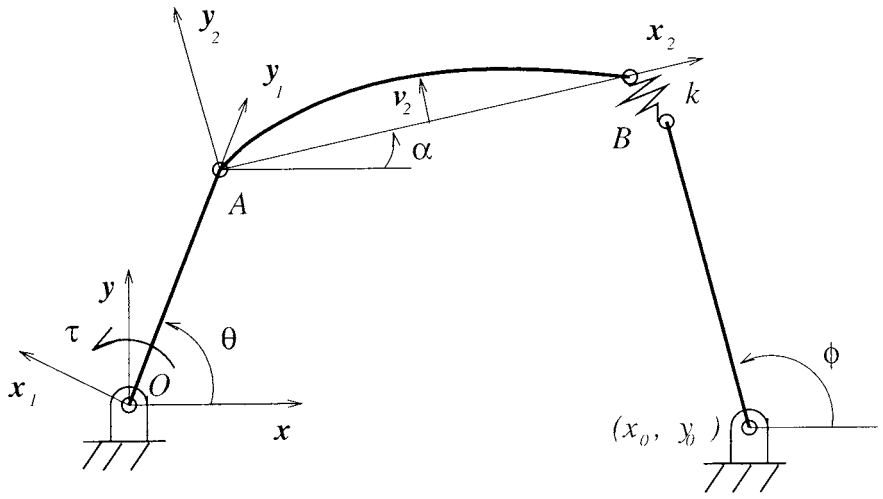

Figure 9. Geometric representation of the four-bar mechanism with a flexible coupler link.

is a very difficult task. The use of virtual springs removes this restriction, and therefore any functions close to these flexural motion of the links (for example polynomial) can be used and ensure good convergence of the results.

The flexible mechanism studied here is represented in Figure 9. The coupler link is considered to be flexible. For simplicity, the virtual link coordinate system [3] or the pinned-pinned boundary condition [4] is chosen (Figure 9) and the Rayleigh–Ritz method is used to discretize the flexible deformation v_2:

$$v_2 = q_{21} \sin\left(\frac{\pi x_2}{l_1}\right) + q_{22} \sin\left(\frac{2\pi x_2}{l_2}\right), \tag{45}$$

where q_{21} and q_{22} are two generalized flexible coordinates.

The position vector of an arbitrary point on the flexible link can be written as

$$\mathbf{p}_{e2} = \mathbf{Q}_1 \mathbf{l}_1 + \mathbf{Q}_2 \mathbf{r}_{e2}, \tag{46}$$

where $\mathbf{Q}_i$, $(i = 1, 2)$ has been previously defined, and

$$\mathbf{l}_1 = \begin{bmatrix} 0 \\ l_1 \end{bmatrix}, \quad \mathbf{r}_{e2} = \begin{bmatrix} x_2 \\ v_2 \end{bmatrix}. \tag{47}$$

Assuming that the flexible link is a thin long bar, its kinetic energy can be expressed as

$$T_2 = \frac{1}{2} \int_0^{l_2} \rho_2 A_2 (\dot{\mathbf{p}}_{e2}^T \dot{\mathbf{p}}_{e2}) \, \mathrm{d}x_2, \tag{48}$$

where ρ_2 is the density of the link and A_2 is its area of section.

The elastic and gravitational potential energy of the link can be written as

$$U_2 = \frac{1}{2} \int_0^{l_2} E_2 I_2 \left(\frac{\mathrm{d}^2 v_2}{\mathrm{d}x_2^2}\right) \mathrm{d}x_2, \tag{49}$$

$$V_2 = \int_0^{l_2} \rho_2 A_2 g (\mathbf{p}_{e2} \cdot \mathbf{j}) \, \mathrm{d}x_2, \tag{50}$$

where $E_2 I_2$ is the bending stiffness of the flexible link.

The kinetic energy and potential energy of the other two moving links as well as the elastic potential energy of the virtual spring are as previously defined for the rigid-link mechanism.

Finally, one can obtain the Lagrangian function

$$L = \sum_{i=1}^{3} (T_i - V_i) - U_2 - V_s. \tag{51}$$

Using the Lagrange formulation, the dynamic equations of the mechanism can then be derived. A system consisting of five ordinary differential equations in five generalized coordinates $\theta, \alpha, \phi, q_{21}$ and q_{22} is obtained. The expressions are not given here because of space limitation.

(II) *Solution of the dynamic model*
It is assumed that all parameters are the same as the ones used in the case of the rigid-link four-bar mechanism studied above except for the flexible coupler link. For the coupler link, the parameters are given as

$$\rho_2 = 12.5 \text{ (kg/m}^3\text{)}, \quad A_2 = 0.02 \text{ (m}^2\text{)},$$

$$E_2 = 2123.56 \text{ (N/m}^2\text{)}, \quad I_2 = 1.333417 \text{ (m}^4\text{)}.$$

Using MAPLE's gear solver with default values for the relative and absolute error tolerances, the forward dynamic solution is obtained. The solution for the displacements and velocities of the three rigid generalized coordinates during the first two seconds are represented in Figure 10 and the relative deflection of the mid-point of the flexible coupler link is shown in Figure 11. It can be noticed that the coupler link undergoes vibration at a dominant frequency which is close to the fundamental frequency of the pinned-pinned beam.

3.2.2. *Comparison of the Results*

The difference between the results obtained with the virtual spring approach and the converted ODE approach are shown in Figure 12. The relative error (in percent) for the deflection of the middle point of the coupler link obtained with the two approaches is represented in Figure 13. It can be seen that the maximum error is about 2%.

3.2.3. *Simulation of Gough–Stewart Platform Using the Virtual Spring Approach*

In this section, the simulation of a Gough–Stewart platform mechanism with a set of given parameters is performed. It is assumed that the actuator torques for the six legs are identical and are represented by the following expressions:

$$\tau_i = 9 \sin(\pi t), \quad i = 1, \ldots, 6$$

and the initial conditions for the generalized coordinates and velocities are given as

$$x = -1.5, \quad y = 0.1, \quad z = 1.5, \quad \phi = 0, \quad \theta = 0.1, \quad \psi = 0,$$

$$\rho_1 = 1.48341, \quad \rho_2 = 1.53551, \quad \rho_3 = 1.66955, \quad \rho_4 = 1.58501,$$

$$\rho_5 = 1.54805, \quad \rho_6 = 1.58566, \quad \alpha_1 = -0.77853, \quad \alpha_2 = -1.31585,$$

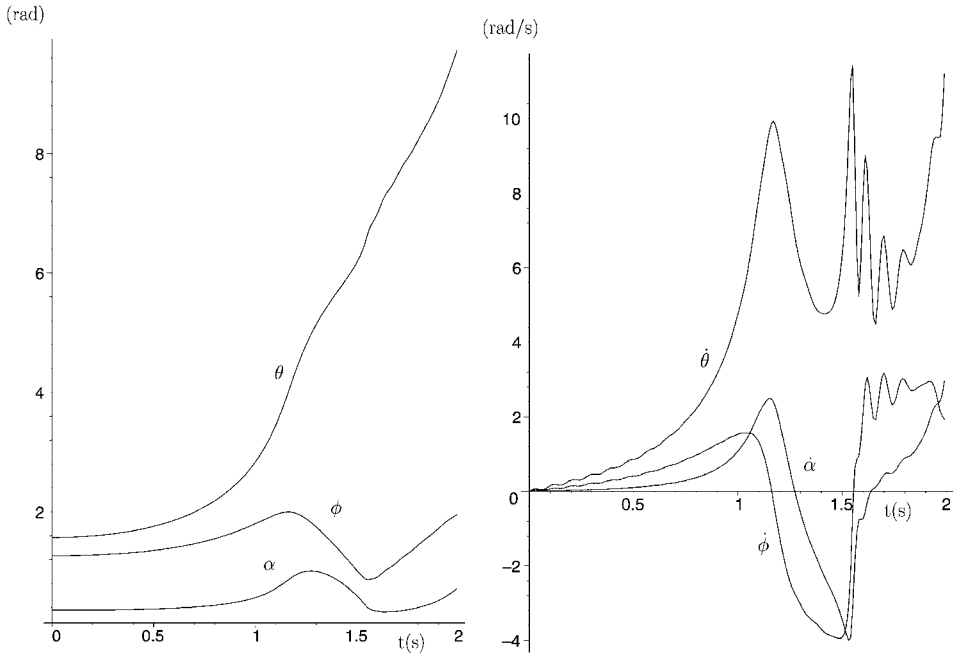

(a) Angular displacements θ, α and ϕ (rad) (b) Angular velocities $\dot{\theta}$, $\dot{\alpha}$ and $\dot{\phi}$ (rad/s)

Figure 10. The angular displacement and velocity of the three links of the four-bar mechanism with the flexible coupler link.

$$\alpha_3 = 1.31585, \quad \alpha_4 = 0.77853, \quad \alpha_5 = -2.87293, \quad \alpha_6 = 2.87293,$$

$$\beta_1 = 1.07521, \quad \beta_2 = 1.07521, \quad \beta_3 = 1.07521, \quad \beta_4 = 1.07521,$$

$$\beta_5 = 1.07521, \quad \beta_6 = 1.07521,$$

$$\dot{x} = 0, \quad \dot{y} = 0, \quad \dot{z} = 0, \quad \dot{\phi} = 0, \quad \dot{\theta} = 0, \quad \dot{\psi} = 0,$$

$$\dot{\rho}_i = \dot{\alpha}_i = \dot{\beta}_i = 0, \quad i = 1, \ldots, 6.$$

The parameters used in this example are given as

$$x_{o1} = -2.120, \quad y_{o1} = 1.374, \quad x_{o2} = -2.380, \; y_{o2} = 1.224,$$

$$x_{o3} = -2.380, \quad y_{o3} = -1.224, \quad x_{o4} = -2.120, \quad y_{o4} = -1.374,$$

$$x_{o5} = 0.0, \quad y_{o5} = -0.15, \quad x_{o6} = 0.0, \quad y_{o6} = 0.15,$$

$$z_{oi} = 0.0 \quad (i = 1, \ldots, 6), \quad a_1 = 0.170, \quad b_1 = 0.595,$$

$$c_1 = -0.4, \quad a_2 = -0.6, \quad b_2 = 0.15, \quad c_2 = -0.4,$$

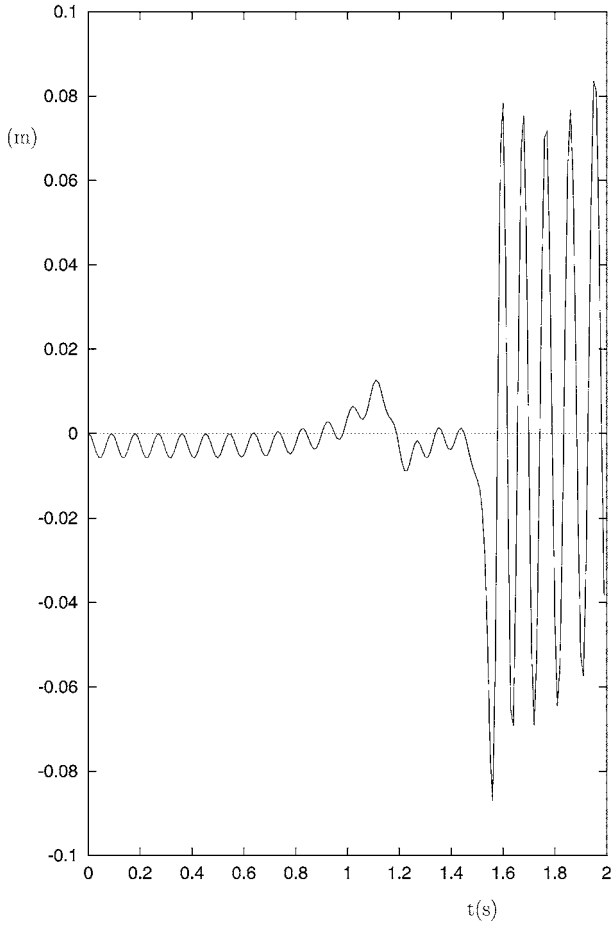

Figure 11. The relative deflection of the mid-point of the coupler link.

$a_3 = -0.6, \quad b_3 = -0.15, \quad c_3 = -0.4, \quad a_4 = 0.170,$

$b_4 = -0.595, \quad c_4 = -0.4, \quad a_5 = 0.430, \quad b_5 = -0.445,$

$c_5 = -0.4, \quad a_6 = 0.430, \quad b_6 = 0.445, \quad c_6 = -0.4,$

$\rho_{i\,\max} = 4.5, \quad \rho_{i\,\min} = 0.5 \quad (i = 1, \ldots, 6),$

$m_p = 1.5, \quad m_{iu} = m_{il} = 0.1, \quad r_{iu} = r_{il} = 0.5 \quad (i = 1, \ldots, 6),$

$\mathbf{r}_p = \mathbf{0}, \mathbf{I}_{iu} = \mathrm{diag}(t,\ t,\ t/10) \quad (i = 1, \ldots, 6),$

$\mathbf{I}_p = \mathrm{diag}(u,\ u,\ u),$

$t = 0.00625, \quad u = 0.08,$

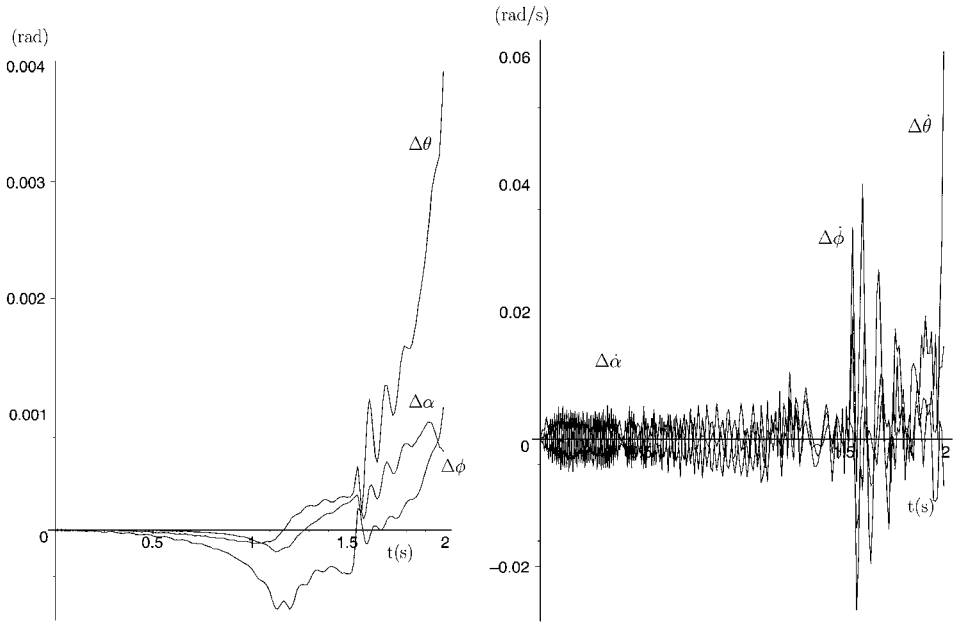

(a) Displacements errors $\Delta\theta$, $\Delta\alpha$ and $\Delta\phi$ (rad) (b) Velocities errors $\Delta\dot{\theta}$, $\Delta\dot{\alpha}$ and $\Delta\dot{\phi}$ (rad/2)

Figure 12. The error curves of the displacement and velocity of the three links of the four-bar mechanism with the flexible coupler link.

where the lengths are given in meters, the masses in kilograms and the inertias in kilograms meter square.

Using MAPLE's gear integration solver with default values for the relative and absolute error tolerances and choosing virtual spring stiffness $k_i = 5 \times 10^4$ and the damping coefficient $b_i = 50$ one can obtain the displacements and velocities of the all moving links of the mechanism.

The simulation results for the Cartesian displacements and velocities of the moving platform during first two seconds are represented in Figure 14. The kinematic constraints of displacements and velocities have been met very well, the errors are around 10^{-4} and 10^{-3} respectively. Because of space limitation, the error plots for the six constraints and the plots for all the other generalized coordinates and velocities are not presented here.

The simulation of the six-degree-of-freedom manipulator has also been performed using Matlab/Simulink and identical results have been obtained. The model consists of seven submodels corresponding to the six legs and the moving platform, therefore, seven processors can be used to run the simulation. For the comparison of implementation time using single and multi-processors, the simulation of the model has respectively been performed in one processor and three processors. A 2 second simulation of the model takes about 6 seconds of computing time using one processor and 0.4 seconds using three processors, namely, the simulation using

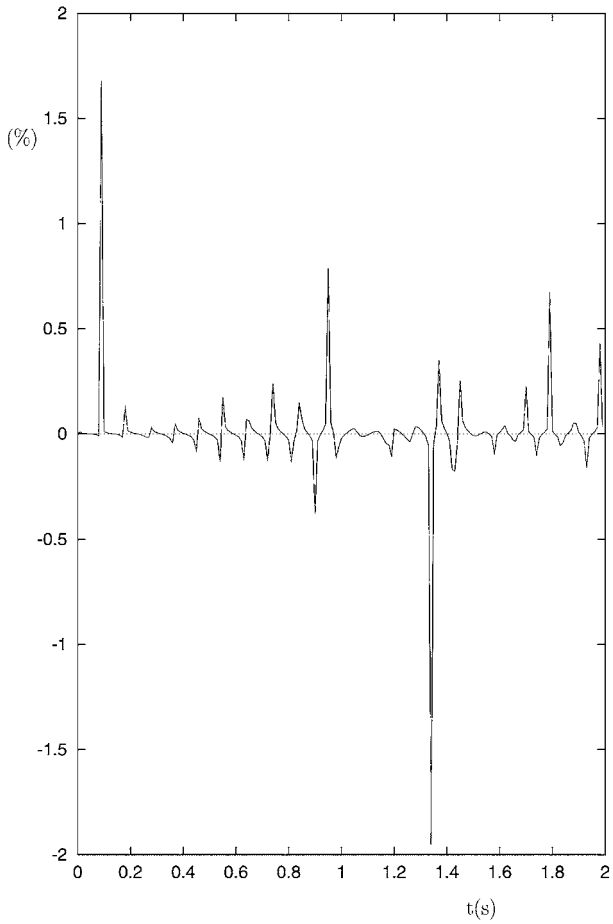

Figure 13. The relative error of the deflection of the mid-point from the results obtained by the two approaches (in percent).

three processors is almost 15 times faster than using only one processor. This is because the time spent for function calling and the idle time of the communication among submodels for the three processors is greatly reduced.

4. Conclusion

The purpose of this paper was to point out the parallel characteristics of the virtual spring approach for the simulation of robotic mechanisms or mechanical systems with closed kinematic chains and to illustrate the advantages of this approach in a context of multi-processor simulation. To demonstrate its feasibility, a simple example – the four-bar mechanism – has first been presented. Then, the modeling and simulation of a well-known parallel mechanism, the Gough–Stewart platform has been performed. It has been noticed that the virtual spring approach can generate

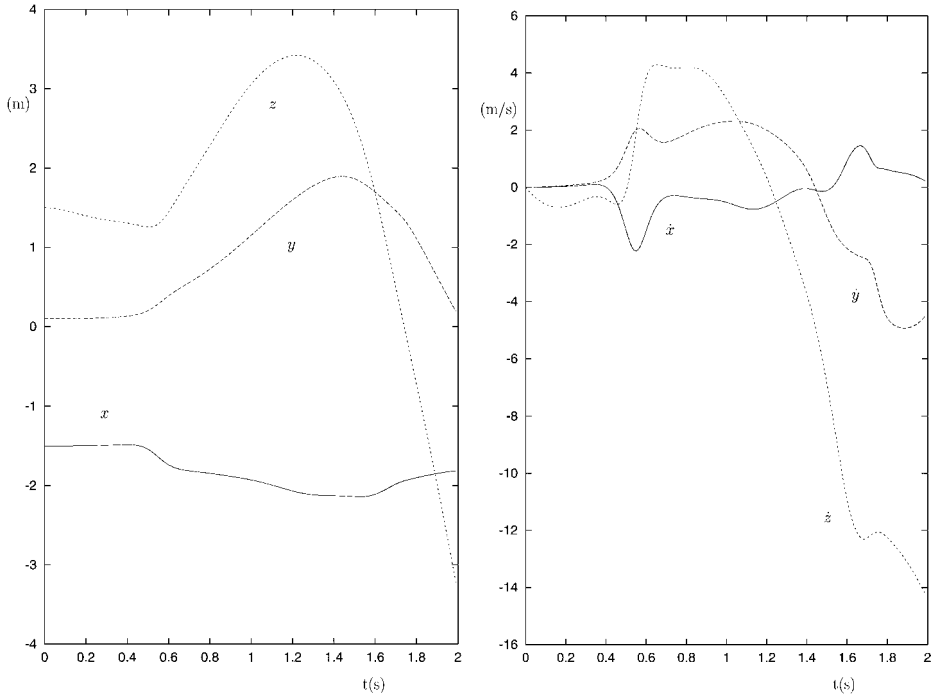

(a) Translational displacement x, y and z (m) (b) Translational velocity V_x, V_y and V_z (m/s)

Figure 14. The translational displacement and velocity along the x, y and z direction.

completely decoupled dynamic models of robotic systems with closed kinematic chains and therefore allows the development of parallel algorithms for real-time simulation using multi-processors. The simulation results obtained with the virtual spring approach have achieved a good agreement with the results obtained from other approaches. Besides, the real-time dynamic simulation of a Gough–Stewart platform has been realized using multi-processors.

References

1. Angeles, J. and Ma, O., 'Dynamic simulation of n-axis serial robotic manipulators using a natural orthogonal complement', *The International Journal of Robotics Research* **7**(5), 1988, 32–47.
2. Armstrong, W.W., 'Recursive solution to the equation of motion of an N-link manipulator', in *Proceedings of the 5th World Congress on the Theory of Machines and Mechanisms*, Montréal, 1979, 1343–1346.
3. Asada, H., Ma, Z.-D. and Tokumaru, H., 'Inverse dynamics of flexible robot arm: Modeling and computation for trajectory control', *ASME Journal of Dynamic Systems, Measurement, and Control* **112**, 1990, 177–185.
4. Book, W.J., 'Controlled motion in an elastic world', *ASME Journal of Dynamic Systems, Measurement, and Control* **115**, 1993, 252–261.

5. Bae, D.-S., Hwang, R.S. and Haug, E.J., 'A recursive formulation for real-time dynamic simulation', in *Proceedings of the ASME Design Automation Conference*, ASME, New York, 1991, 499–508.
6. Bhattacharya, S., Nenchev, D. and Uchiyama, M., 'A recursive formula for the inverse of the inertia matrix of a parallel manipulator', *Mechanism and Machine Theory* **33**(7), 1998, 957–964.
7. Chung, S. and Haug, E.J., 'Real-time simulation of multibody dynamics on shared memory multiprocessors', *ASME Journal of Dynamic Systems, Measurement, and Control* **115**, 1993, 627–637.
8. Cheng, L., 'Vibroacoustic modeling of mechanically coupled structures: Artificial spring technique applied to light and heavy mediums', *Journal of Shock and Vibration* **3**(3), 1996, 193–200.
9. Dasgupta, B. and Mruthyunjaya, T.S., 'Closed-form dynamic equations of the general Stewart platform through the Newton-Euler approach', *Mechanism and Machine Theory* **33**(7), 1983, 993–1102.
10. Eich-Soellner, E. and Fuhrer, C., *Numerical Methods in Multibody Dynamics*, Teubner, Stuttgart, 1998.
11. Fuhrer, C. and Leimkuhler, B.J., 'Numerical solution of differential-algebraic equations for constrained mechanical motion', *Numerische Mathematik* **59**, 1991, 55–69.
12. Featherstone, R., 'The calculation of robot dynamics using articulated-body inertias', *The International Journal of Robotics Research* **2**(1), 1983, 13–30.
13. Garcia de Jalon, J. and Bayo, E., *Kinematic and Dynamic Simulation of Multibody Systems: The Real-Time Challenge*, Springer-Verlag, Berlin, 1998.
14. Kecskeméthy, A., Krupp, T. and Hiller, M., 'Symbolic processing of multiloop mechanism dynamics using closed-form kinematic solutions', *Multibody System Dynamics* **1**(1), 1997, 23–45.
15. Lee, C.S.G. and Chang, P.R., 'Efficient parallel algorithms for robot forward dynamics computation', *IEEE Transactions on System, Man, and Cybernetics* **18**(2), 1988, 238–251.
16. Petzold, L.R., Jay, L.O. and Yen, J., 'Numerical solution of highly oscillatory ordinary differential equations', *Acta Numerica* **6**, 1997, 437–484.
17. Piedboeuf, J.-C., 'Symbolic modelling of flexible manipulators', in *Proceedings AAS/AIAA Astrodynamics Specialist Conference*, Halifax, Canada, AAS, San Diego, 1995, 1–20.
18. Pond, B. and Sharf, I., 'Dynamics simulation of multibody chains on a transputer system', *Concurrency: Practice and Experience* **8**(3), 1996, 235–249.
19. Yuan, J. and Dickinson, S.M., 'On the use of artifical springs in the study of the free vibrations of systems comprised of straight and curved beams', *Journal of Sound and Vibration* **153**, 1992, 203–216.
20. Schiehlen, W., Rukgauer, A. and Schirle, Th., 'Force coupling versus differential algebraic description of constrained multibody systems', *Multibody System Dynamics* **4**, 2000, 317–340.
21. Sharf, I. and D'Eleuterio, G.M.T., 'Parallel simulation dynamics for elastic multibody chains', *IEEE Transactions on Robotics and Automation* **8**(5), 1992, 597–606.
22. Shi, P. and McPhee, J., 'Dynamics of flexible multibody systems', *Multibody System Dynamics* **4**, 2000, 355–381.
23. Shi, P., 'Flexible multibody dynamics: A new approach using virtual work and graph theory', Ph.D. Thesis, The University of Waterloo, Canada, 1998.
24. Wang, J. and Gosselin, C., 'Dynamic modeling and simulation of parallel mechanisms using the virtual spring approach', in *Proceedings of 2000 ASME Design Engineering Technical Conferences*, Baltimore, MD, ASME, New York, 2000.
25. Wang, J. and Gosselin, C., 'Parallel computational algorithms for the simulation of closed-loop robotic systems', in *Proceedings IEEE International Conference on Parallel Computing in Electrical Engineering*, Trois-Rivieres, Quebec, IEEE, Los Alamitos, 2000, 34–38.

26. Wang, J. and Gosselin C.M., 'A new approach for the dynamic analysis of parallel manipulators', *Multibody System Dynamics* **2**(3), 1998, 317–334.
27. Walker, M.W. and Orin, D.E., 'Efficient dynamic computer simulation of robotic mechanisms', *ASME Journal of Dynamic Systems, Measurement, and Control* **104**, 1982, 205–211.
28. Yoshikawa, T. and Hosoda, K., 'Modeling of flexible manipulator using virtual rigid links and passive joints', *International Journal of Robotics Research* **15**(3), 1996, 290–299.